

## Crystal Structure and Magnetic Susceptibility of Iron Sand From Pangeo Village, Morotai Jaya Subdistrict as The Cathode of Lithium-Ion Batteries

Rahim Achmad<sup>1</sup>, Suryani Taib<sup>2\*</sup>, Rohima Wahyu Ningrum<sup>3</sup>

<sup>1</sup> Department of Physics Education, Universitas Khairun, Indonesia, [rahim.achmad@unkhair.ac.id](mailto:rahim.achmad@unkhair.ac.id)

<sup>2</sup> Department of Physics Education, Universitas Khairun, Indonesia, [ryanitaib@gmail.com](mailto:ryanitaib@gmail.com)

<sup>3</sup> Department of Physics Education, Universitas Khairun, Indonesia, [rohima@unkhair.ac.id](mailto:rohima@unkhair.ac.id)

Received : 18-08-2022

Accepted : 25-09-2022

Available online : 30-10-2022

### ABSTRACT

Morotai Island has a wealth of iron sand which is a natural resource in Morotai Jaya District, Pangeo Village. The utilization of iron sand is still for local community building materials. The purpose of this study was to determine the structure and magnetic susceptibility of iron sand as a basic material for cathode materials in the manufacture of lithium-ion batteries (LIB). The research sample was taken randomly, then it was prepared in the laboratory to obtain dry-phase iron sand. After being tested using an XRD tool, namely samples A, E, and I, it was found that there was a lot of  $\text{Fe}_3\text{O}_4$  contained in iron sand. The diffraction peaks indicate  $\text{Fe}_3\text{O}_4$  material with an inverse spinel structure. Sample A is the most crystalline compared to sample I. Sample E has the lowest diffraction peak pattern due to the dominant mineral hematite ( $\text{Fe}_2\text{O}_3$ ) 70.31%. The value of the BSM test obtained the greatest magnetic susceptibility of  $82867.54 \times 10^{-8} \text{m}^3/\text{kg}$ . The smallest is in sample J with a value of  $13186.98 \times 10^{-8} \text{m}^3/\text{kg}$  because during synthesis it is slightly attracted by magnets and the color is not too black which mixes a lot with other materials. In addition, this relationship is directly proportional to sample E which contains the magnetic material  $\text{Fe}_2\text{O}_3$  of the characterization of 70.31. The range of magnetic susceptibility values in samples A to L is in the interval  $(46 - 80,000) \times 10^{-8} \text{m}^3/\text{kg}$ , and  $(20,000 - 110,000) \times 10^{-8} \text{m}^3/\text{kg}$ . Based on this interval, both magnetic and mass susceptibility of each iron sand sample contained ilmenite ( $\text{FeTiO}_3$ ) particles in the antiferromagnetic group and magnetite ( $\text{Fe}_3\text{O}_4$ ) in the ferromagnetic group.

Keywords: Crystal structure, Iron sand, magnetic susceptibility

### ABSTRAK

Pulau Morotai memiliki kekayaan pasir besi yang merupakan sumber daya alam di Kecamatan Morotai Jaya, Desa Pangeo. Pemanfaatan pasir besi tersebut masih untuk bahan bangunan masyarakat setempat. Tujuan penelitian ini adalah menentukan Struktur Dan Suseptibilitas Magnetik Pasir Besi sebagai bahan dasar untuk Material Katoda dalam pembuatan Baterai Lithium Ion (LIB). Sampel penelitian diambil secara random, kemudian dilakukan preparasi di laboratorium untuk mendapatkan pasir besi fasa kering. Setelah diuji dengan menggunakan alat XRD yaitu sampel A, E, I. didapatkan kandungan  $\text{Fe}_3\text{O}_4$  banyak terkandung dalam pasir besi. Puncak-puncak difraksi menunjukkan material  $\text{Fe}_3\text{O}_4$  dengan struktur invers spinel. Sampel A paling kristalin dibandingkan dengan sampel I. Sampel E memiliki pola puncak difraksi paling rendah karena dominannya mineral hematite ( $\text{Fe}_2\text{O}_3$ ) 70,31%. Nilai dari uji BSM didapatkan suseptibilitas magnetik terbesar  $82867,54 \times 10^{-8} \text{m}^3/\text{kg}$ . Paling terkecil ada di sampel J dengan nilai  $13186,98 \times 10^{-8} \text{m}^3/\text{kg}$  karena saat sintesis sedikit ditarik magnet dan warnanya tidak terlalu hitam yang banyak bercampur dengan material lainnya. Selain itu, hubungan ini berbanding lurus dengan sampel E yang memiliki kandungan material magnetik  $\text{Fe}_2\text{O}_3$  dari karakterisasi sebesar 70,31. Rentang nilai suseptibilitas magnetik pada sampel A sampai L berada pada interval (46-

80000)  $\times 10^{-8}$  m<sup>3</sup>/kg, dan (20.000-110.000)  $\times 10^{-8}$  m<sup>3</sup>/kg. Berdasarkan interval tersebut suseptibilitas baik magnetik maupun massa dari tiap sampel pasir besi mengandung partikel ilmenit (FeTiO<sub>3</sub>) pada grup antiferomagnetik, serta magnetite (Fe<sub>3</sub>O<sub>4</sub>) berada di grup feromagnetik.

Kata kunci: Pasir besi, Struktur kristal, Suseptibilitas magnetik

## INTRODUCTION

Lithium battery has been widely recognized as an electricity storage device that is widely applied in various electronic equipment. The characteristics of the battery (LiFePO<sub>4</sub>), are stable, cheap, and cycle stability with an abundance of raw materials (Steward *et al.*, 2019; Shen & Liu, 2021). According to (Wang *et al.*, 2022), lithium batteries still have economic value, in recycling. But, according to (Zhang *et al.*, 2020; Paniyarasi *et al.*, 2021; Ahsan *et al.*, 2021; Li *et al.*, 2022; Yang *et al.*, 2021), LiFePO<sub>4</sub> has a weakness in electrochemical performance which inhibits battery power. To overcome this, it is necessary to review the doping modification.

Many studies on magnetic materials have been carried out, especially magnetic nanoparticles for applications such as Ferrofluids (Saputro *et al.*, 2019; Afkhami & Renardy, 2017), humidity sensors (Khorsand *et al.*, 2020), Magnetic Resonance Imaging (MRI) (Zhou *et al.*, 2022) and many more. Some natural materials contain this magnetic material, such as iron sand. According to (Haryati *et al.*, 2021; Sadjab *et al.*, 2020; Togibasa *et al.*, 2018), the main content of iron sand is Fe in the bonds of mineral oxides such as magnetite (Fe<sub>3</sub>O<sub>4</sub>), hematite ( $\alpha$ -Fe<sub>2</sub>O<sub>3</sub>), and maghemite ( $\gamma$ -Fe<sub>2</sub>O<sub>3</sub>). Other minerals such as aluminum oxide (Al<sub>2</sub>O<sub>3</sub>), silica dioxide (SiO<sub>2</sub>), phosphorus pentoxide (P<sub>2</sub>O<sub>5</sub>), calcium oxide (CaO), titanium dioxide (TiO<sub>2</sub>), vanadium pentoxide (V<sub>2</sub>O<sub>5</sub>), chromium (iii) oxide (Cr<sub>2</sub>O<sub>3</sub>). (Malega *et al.*, 2018), have also examined the content of manganese oxide (MnO) in iron sand.

Ferrite is an attractive material because of its unique properties, such as high thermal permeability and low resistivity and coercivity (Setiadi *et al.*, 2018). Ferrite is known as a soft magnetic material that has a spinel structure. The chemical formula for a ferrite is M-Fe<sub>2</sub>O<sub>4</sub>, where M is a divalent metal ion, such as Cu, Zn, Ni, Co, Fe, Mn, and Mg. In addition, ferrite materials have strong mechanical properties, and high stability in external fields and temperatures (Khuriati, 2004). Minerals in sand iron are very useful for many applications, such as component fabrication for electronic devices, manufacturing, the construction sector, buildings, industrial vehicles as well as for the automotive sector.

North Mollucas with its geological setting, causes there are many mineral deposits. The availability of certain minerals is closely related to the occurrence process and the way it is deposited. Many of these iron sand deposits are distributed from the northern part of Halamahera Island to Morotai Island, especially in the northern part of Morotai Island (Lamburu *et al.*, 2017; Sadjab *et al.*, 2020; Malega *et al.*, 2018; Endang *et al.*, 2021). Iron sand is scattered along the coast but has not been explored. Residents around the coast use iron sand to make buildings. Quality Iron sand contains a lot of magnetite, ilmenite, and iron oxide which is formed due to the destruction of the original rock by weather, and tide waves. This iron sand is usually dark gray or black in color (Nengsi, 2016; Nurrohman *et al.*, 2018).

This research aims to examine the crystal structure, susceptibility, and mineral content of iron sand in Pangeo Village, Morotai Jaya District as the basic material for cathode materials in the manufacture of Lithium Ion batteries. Microscopic rock observations will provide information to complement the initial data for the exploration of iron sands. Iron sand was characterized by XRF (X-Ray Fluorescence) to determine its mineral content. After that, it was characterized by

XRD (X-Ray Diffractometer) to determine the structure and size of the particles and BMSM (Bartington Magnetic Susceptibility Meter) to measure the magnetic susceptibility of iron sand.

## METHODOLOGY

### Sample Site

our research samples were taken along the coast every 100 m. The sampling map is shown in Figure 1. Sampling was only focused on Pangeo village because the sand deposits are thicker. The sampling area is shown in figure 2.

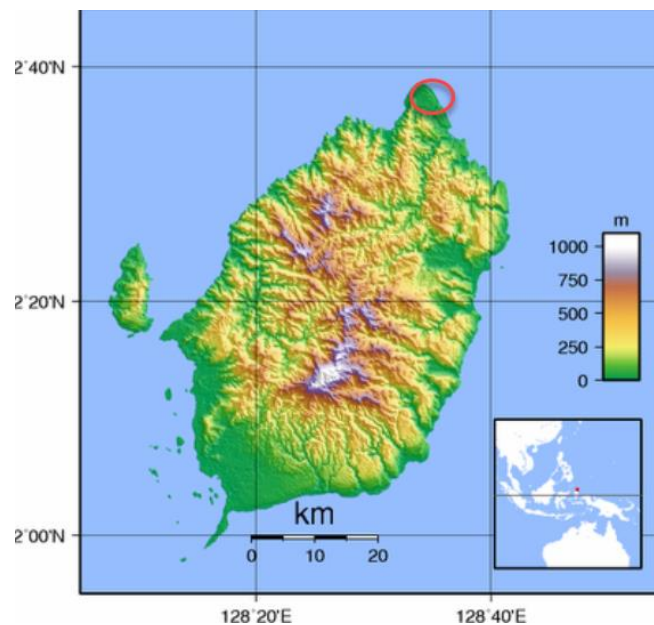


Figure 1. Morotai Island and the sampling site



Figure 2. A sampling of iron sand

### Sample Preparation

The iron sand sample is crushed to separate it from ordinary sand using a permanent magnet. After being separated, 60 gr of samples A, E, and I were taken, while for samples B, C, D, F, G, H, J, K, and L each 30 gr. samples A, E, I were used for the XRF, XRD, and Barrington Susceptibility Meter tests. The samples were soaked in 70% ethanol for 2 hours, then placed on

the fire. Furthermore, washing 15 minutes 10 times to reduce unwanted residue during characterization with 60 ml of Aquades for A, E, and I and 30 ml for other samples. The samples were then dried at 100°C until dry. The sample preparation process is shown in Figure 3.



Figure 3. Sample preparation process

## RESULTS AND DISCUSSION

The elemental compositions of the iron sand samples analyzed using X-ray fluorescence were shown in Table 1. The Fe element is the most dominant magnetic element, together with a small composition of other transition elements which also have magnetic properties, such as Si, Ca, Mn, and Ti. (Haryati et al., 2021; Togibasa et al., 2018). The non-magnetic Si element is the second dominant element, followed by the Ca, Ti, and Mn elements. Overall, this composition shows the typical characteristic type of natural iron sand. The average percentage content of all elements are: Fe<sub>2</sub>O<sub>3</sub> (58,6%), SiO<sub>2</sub> (21,1%), CaO (8,2%), TiO<sub>2</sub> (5,2%), MnO (1,3)%

Table 1. Percentage of elements

Sample Code	Fe <sub>2</sub> O <sub>3</sub>	SiO <sub>2</sub>	CaO	TiO <sub>2</sub>	MnO
A	50.94%	29.29%	13.10%	5.10%	1.29%
E	70.31%	15.47%	6.10%	5.19%	1.44%
I	54.58%	18.40%	5.45%	5.26%	1.18%

The structural results of the Fe<sub>2</sub>O<sub>4</sub> and Fe<sub>2</sub>O<sub>3</sub> particles analyzed by XRD patterns are shown in Fig. 4 and Table 2. The results of the XRD characterization show the structural particle of each sample. As an example for sample A, it is seen the diffraction peaks which represent the Miller index in fields (220), (311), (400), (511), and (440) are the diffraction peaks of the Fe<sub>3</sub>O<sub>4</sub> material with an inverse spinel structure according to the JCPDS standard data (ICDD Card No: 19-0629). As seen in Figure 1, the peaks are mainly 311 highest in sample A so it is more crystalline compared to sample I, but not in sample E has a different diffraction pattern d. This is due to the dominance of other hematite (Fe<sub>2</sub>O<sub>3</sub>) minerals so that when synthesis is more oxidized.

The total magnetic and mass susceptibility values of each sample differ depending on the sample's field strength. The difference in the values of magnetic susceptibility and mass susceptibility is caused by differences in the number of magnetic minerals in soil deposits (Yulianto et al., 2003; Haryati et al., 2021; Sebayang et al., 2022; Togibasa et al., 2018). As shown in Table 2, the 12 samples have very varying mass magnetic susceptibility values.

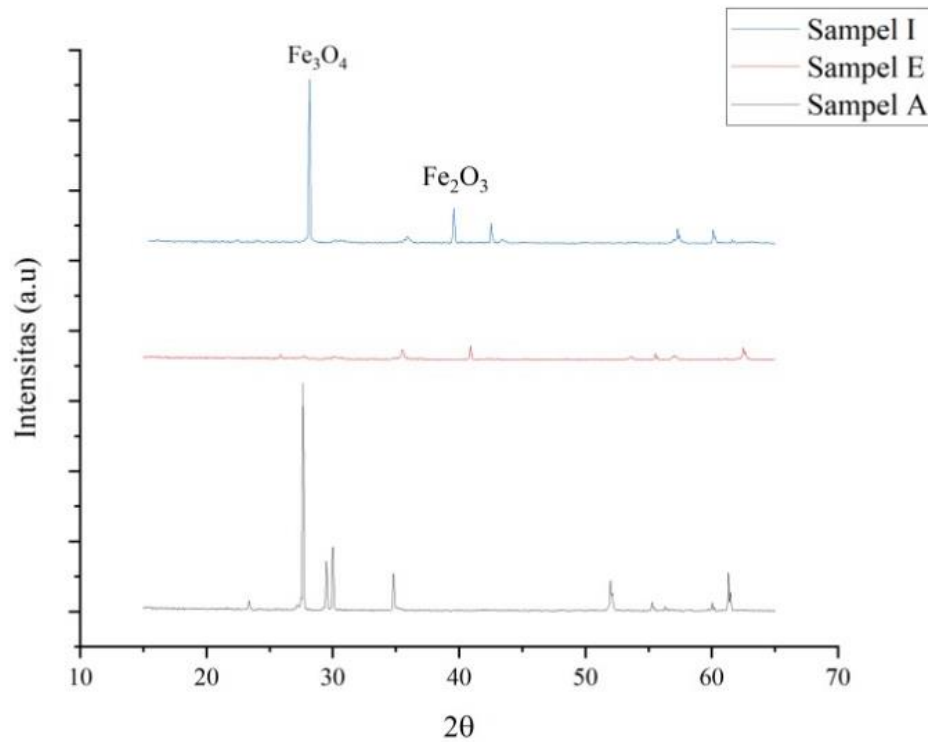


Figure 4. XRD patterns of samples

Table 2. Magnetic Susceptibility of the iron sand sample

Sample Code	Total Magnetic	Susceptibility Mass ( $10^{-8} \text{ m}^3/\text{kg}$ )
A	12,63	13965,42
B	12,63	32583,40
C	12,63	19501,98
D	12,62	42074,24
E	<b>12,64</b>	<b>82867,54</b>
F	12,64	54803,13
G	12,63	51206,92
H	12,62	64797,60
I	12,61	41215,42
J	12,63	13186,98
K	12,67	67256,70
L	12,63	81296,68

In Table 2, it can be seen that the highest magnetic susceptibility value is found in sample E ( $82867 \times 10^{-8} \text{ m}^3/\text{kg}$ ), and the smallest is in sample J ( $13186.98 \times 10^{-8} \text{ m}^3/\text{kg}$ ). This is because the J sample is not magnetically attracted too much, and the color is not very black. Sample E is most easily attracted by a magnet. This is consistent with the  $\text{Fe}_2\text{O}_3$  content of sample E (70.31%). The greater the magnetic susceptibility value, the greater the content of the magnetic mineral  $\text{Fe}_2\text{O}_3$  which is the basic material for the cathode in the manufacture of lithium-ion batteries. (Shen & Liu, 2021; Wang *et al.*, 2022; Sun *et al.*, 2022).

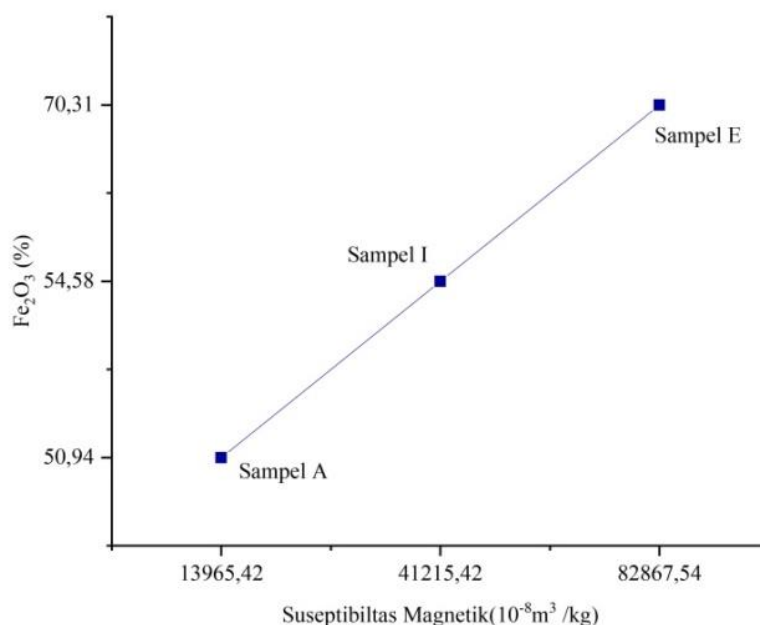


Figure 5. Suseptibilitas relationship with  $\text{Fe}_2\text{O}_3$  magentic material content

The range of magnetic susceptibility values in samples A to L is in the interval (46 - 80.000)  $\times 10^{-8} \text{ m}^3/\text{kg}$ , and (20.000 - 110.000)  $\times 10^{-8} \text{ m}^3/\text{kg}$ . Based on this interval, both the magnetic reliability and the mass of each iron sand sample contain ilmenite ( $\text{FeTiO}_3$ ) particles in the antiferromagnetic group, and magnetite ( $\text{Fe}_3\text{O}_4$ ) in the ferromagnetic group.

## CONCLUSION

The material content obtained from Pangeo Village Iron Sand is illuminated by magnetic materials  $\text{Fe}_3\text{O}_4$  and  $\text{Fe}_2\text{O}_3$ . The crystal structure of the spinner inverse crystal with the greatest christianity is found in sample A. Based on the degree of magnetism of soil deposits found along the Sail river it is known that the spread of magnetic content is getting higher (46-80000)  $\times 10^{-8} \text{ m}^3/\text{kg}$ , and (20,000-110,000)  $\times 10^{-8} \text{ m}^3/\text{kg}$ . Based on these intervals, both magnetic and mass reliability of each iron sand sample contains ilmenite particles ( $\text{FeTiO}_3$ ) in the antiferromagnetic group, and magnetite ( $\text{Fe}_3\text{O}_4$ ) is in the ferromagnetic group.

## ACKNOWLEDGEMENTS

The authors This research was fully funded by the DIPA UNKHAIR, through PUPKT 2021 (Contract Number: 012/PUPKT/PG.12/2021).

## REFERENCES

- Afkhami, S., & Renardy, Y. (2017). Ferrofluids and Magnetically Guided Superparamagnetic Particles in Flows: A Review of Simulations And Modeling. *Journal of Engineering Mathematics*, 107(1), 231-251. <https://doi.org/10.1007/s10665-017-9931-9>
- Ahsan, Z., Ding, B., Cai, Z., Wen, C., Yang, W., Ma, Y., & Zhang, S. (2021). Recent Progress in Capacity Enhancement of Lifepo4cathode for Li-Ion Batteries. *Journal of Electrochemical Energy Conversion and Storage*, 18(1). <https://doi.org/10.1115/1.4047222>

- Haryati, E., Dahlan, K., Bunga, M., Napitupulu, D., & Togibasa, O. (2021). Mineral Content and Magnetic Properties of River Iron Sand from Jayapura, Papua. *Journal of Magnetism and Its Applications*, 1(2), 30–33. <https://doi.org/10.53533/jma.v1i2.13>
- Khorsand Zak, A., Shirmahd, H., Mohammadi, S., & Banihashemian, S. M. (2020). Solvothermal Synthesis of Porous Fe<sub>3</sub>O<sub>4</sub> Nanoparticles for Humidity Sensor Application. *Materials Research Express*, 7(2), 1–10. <https://doi.org/10.1088/2053-1591/ab6e3c>
- Lamburu, A. A., Syafri, I., Yuningsih, E. T., and Utara, H. (2017). Karakteristik Mineralogi Endapan Pasir Besi di Daerah Galela Utara Kabupaten Halmahera Utara Provinsi Maluku Utara. *Bulletin of Scientific Contribution*, 15(2), 151–160. <https://doi.org/10.24198/bsc%20geology.v15i2.13395>
- Malega, F., Indrayana, I. P. T., & Suharyadi, E. (2018). Synthesis and Characterization of The Microstructure and Functional Group Bond of Fe<sub>3</sub>O<sub>4</sub> Nanoparticles from Natural Iron Sand in Tobelo North Halmahera. *Jurnal Ilmiah Pendidikan Fisika Al-Biruni*, 7(2), 13–22. <https://doi.org/10.24042/jipfalbiruni.v7i2.2913>
- Paniyarasi, S. A. S., Suja, S. K., & Elizabeth, R. N. (2021). Doping and Surface Modification Enhance the Applicability of Nanostructured Fullerene–MWCNT Hybrid Draped LiNi<sub>0.1</sub>Mg<sub>0.1</sub>Co<sub>0.8</sub>O<sub>2</sub> as High Efficient Cathode Material for Lithium-Ion Batteries. *Journal of Inorganic and Organometallic Polymers and Materials*, 31(10), 3976–3990. <https://doi.org/10.1007/s10904-021-02039-5>
- Sadjab, B. A., Indrayana, I. P. T., Iwamony, S., & Umam, R. (2020). Investigation of The Distribution and Fe Content of Iron Sand at Wari Ino Beach Tobelo Using Resistivity Method with Werner-Schlumberger Configuration. *Jurnal Ilmiah Pendidikan Fisika Al-Biruni*, 9(1), 141–160. <https://doi.org/10.24042/jipfalbiruni.v9i1.5394>
- Saputro, R. E., Taufiq, A., Hidayat, N., Sunaryono, Hariyanto, Y. A., & Hidayat, A. (2019). Preparation of Fe<sub>3</sub>O<sub>4</sub>/OA/DMSO Ferrofluids using a Double Surfactant System as Antifungal Materials Candidate. *IOP Conference Series: Materials Science and Engineering*, 515(1). <https://doi.org/10.1088/1757-899X/515/1/012029>
- Sebayang, A. M. S., Rianna, M., Sagala, L. P. S., Asri, N. S., Tetuko, A. P., Setiadi, E. A., Nurdiyansah, L. F., Amiruddin, E., Sembiring, T., & Sebayang, P. (2022). Nanostructures and magnetic properties of Zn<sub>1-x</sub>Cu<sub>x</sub>/2Ni<sub>x</sub>/2Fe<sub>2</sub>O<sub>4</sub> (x = 0-0.4) synthesized from natural iron sand. *South African Journal of Chemical Engineering*, 42(August), 216–222. <https://doi.org/10.1016/j.sajce.2022.08.013>
- Shen, F., & Liu, Y. (2021). LiFePO<sub>4</sub> Cathode Material Modification and its Recycling Research Based on The Development Status of Lithium-Ion Batteries. *Academic Journal of Environment & Earth Science*, 3(3), 4–8. <https://doi.org/10.25236/ajee.2021.030302>
- Steward, D., Mayyas, A., & Mann, M. (2019). Economics and Challenges of Li-Ion Battery Recycling from End-Of-Life Vehicles. *Procedia Manufacturing*, 33, 272–279. <https://doi.org/10.1016/j.promfg.2019.04.033>
- Togibasa, O., Bijaksana, S., & Novala, G. C. (2018). Magnetic Properties of Iron Sand from The Tor River Estuary, Sarmi, Papua. *Geosciences (Switzerland)*, 8(4). <https://doi.org/10.3390/geosciences8040113>
- Wang, M., Liu, K., Yu, J., Zhang, C.-C., Zhang, Z., & Tan, Q. (2022). Recycling Spent Lithium-Ion Batteries Using A Mechanochemical Approach. *Circular Economy*, 1(2), 100012. <https://doi.org/10.1016/j.cec.2022.100012>
- Yang, G., Pan, K., Lai, F., Wang, Z., Chu, Y., Yang, S., ... & Li, Q. (2021). Integrated Co-Modification of PO<sub>4</sub><sup>3-</sup> Polyanion Doping and Li<sub>2</sub>TiO<sub>3</sub> Coating for Ni-Rich Layered Lini<sub>0.6</sub>Co<sub>0.2</sub>Mn<sub>0.2</sub>O<sub>2</sub> Cathode Material of Lithium-Ion Batteries. *Chemical Engineering Journal*, 421, 129964. <https://doi.org/10.1016/j.cej.2021.129964>

- Sun, Y. Q., Luo, X. T., Zhu, Y. S., Liao, X. J., & Li, C. J. (2022). Li<sub>3</sub>PO<sub>4</sub> electrolyte of high conductivity for all-solid-state lithium battery prepared by plasma spray. *Journal of the European Ceramic Society*, 42(10), 4239-4247. <https://doi.org/10.1016/j.jeurceramsoc.2022.04.010>
- Yulianto, A., Bijaksana, S., & Loeksmanto, W. (2003). Comparative Study on Magnetic Characterization of Iron Sand from Several Locations in Central Java. *Indonesian Journal of Physics*, 14(2), 63-66.
- Zhang, H., Zou, Z., Zhang, S., Liu, J., & Zhong, S. (2020). A review of the Doping Modification of LiFePO<sub>4</sub> as a Cathode Material for Lithium Ion Batteries. *International Journal of Electrochemical Science*, 15, 12041-12067. <https://doi.org/10.20964/2020.12.71>
- Zhou, Y., Chen, P., Chen, M., Li, J., Li, X., Lin, L., Lun, Y., Li, Q., Xiao, Q., Huang, Y., Wang, X., Zou, H., & Ye, G. (2022).  $\gamma$ -Fe<sub>2</sub>O<sub>3</sub>@Poly(sucrose allyl ether) Magnetic Microspheres for Tumor Enhanced Magnetic Resonance Imaging and High-Efficiency Cooperative Magnetothermal Therapy. *Materials and Design*, 222, 111062. <https://doi.org/10.1016/j.matdes.2022.111062>